Proceedings of "Applications of Physics in Mechanical and Material Engineering" (APMME 2023)

Comparing C_3N and C_3B Anode Materials with Graphene Using DFT Calculations

G.T. Kasprzak*

Institute of Physics, Czestochowa University of Technology, Armii Krajowej Ave. 19, 42-200 Częstochowa, Poland

Doi: 10.12693/APhysPolA.144.402 *e-mail: grzegorz.kasprzak@pcz.pl

The growing demand for lithium, which is essential for the production of batteries, has led to a significant rise in the price of lithium. The quest for novel materials that could enhance battery performance has thus become a key challenge for scientists. In this regard, the author conducted a comparative analysis of materials based on graphene, using density functional theory and *ab initio* molecular dynamics methods. The materials considered for comparison include graphene, C_3B, and C_3N. For the calculations, two-layer systems of pristine graphene and graphene modified by substituting carbon atoms with boron and nitrogen were constructed. The stability of these systems was examined using the Quantum Espresso and CP2K software at 0 K and 300 K, respectively. In the search for an alternative to lithium, systems incorporating sodium and lithium intercalated between graphene layers were also included in the comparison.

topics: C_3N, C_3B and graphene, electronic properties, electrode materials, density functional theory (DFT) calculations

1. Introduction

The use of density functional theory (DFT) calculations has increasingly demonstrated its efficacy across various scientific domains, encompassing the modeling of biological systems and the exploration of novel superconductors [1, 2], and the identification of anode materials [3, 4]. In the pursuit of discovering new materials, two-dimensional materials have garnered significant attention. Notably, graphene [5], phosphorene [6–8], borophene [9], silicene [10], among others, have emerged as the most prominent examples. Employing atomic-scale modeling facilitates the exceptional opportunity to investigate and assess the stability of materials. In this study, a comparative analysis was conducted on pristine graphene and C_3N and C_3B — two graphene-like structures. The examination of the C_3N bilayer serves as a continuation of previous research on the C_3N monolayer, employing first-principles DFT calculations [11]. Notably, the study reveals the preference of Li and Na atoms to occupy the hollow sites. Within this article, comparative investigation of graphene-based materials will be presented. *Ab initio* molecular dynamics (AIMD) calculations were applied to single- and double-layer C_3B, graphene, and C_3N systems. The exploration of graphene materials is undertaken within the context of their potential as electrode materials in batteries. Hence, a comparison of these materials' properties, specifically with regard to the incorporation of lithium and sodium ions, is indispensable. The Quantum Espresso (QE) program was utilized to calculate the geometric aspects of the structures, while the CP2K program assessed their stability at a temperature of 300 K.

2. Computational methods

To study the electronic properties of the investigated material, first-principles calculations are performed within the framework of density-functional theory (DFT) [12] as implemented in the Quantum Espresso package [13]. The generalized gradient approximation of Perdew–Burke–Ernzerhof (GGA-PBE) is used for the exchange-correlation functional together with the projector-augmented wave (PAW) method. A vacuum of 20 Å was applied along the z-axis to prevent interlayer interactions from the periodic images. Van der Waals forces were taken into account in the simulation. Values of ecutrho = 50, ecutwfc = 500 and k-points = $(18, 18, 1)$ in the QE calculations were taken. Figure 1 shows the visualization of the investigated bilayer structures.

3. Results and discussion

The crystal structure of the C_3B, graphene, and C_3N monolayer has $P6/mmm$ symmetry with a hexagonal lattice. As with graphene, C_3B and C_3N

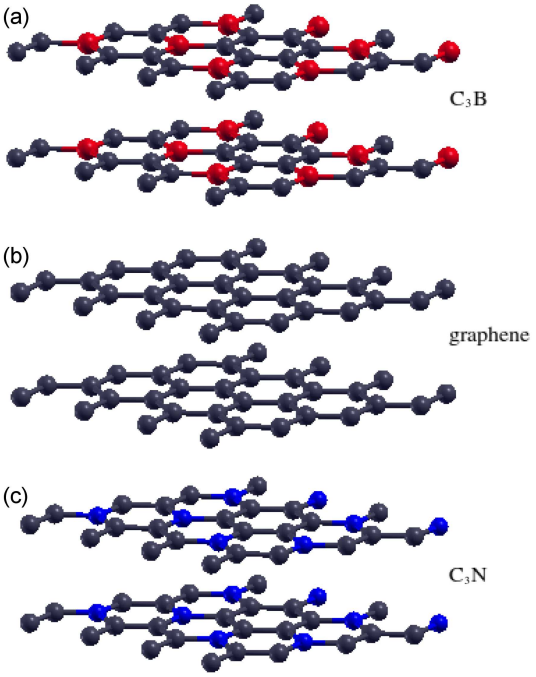

Fig. 1. Visualization of investigated bilayer materials: (a) C_3B, (b) graphene, and (c) C_3N.

have a flat structure because all B, C, and N atoms are sp^2 hybridized. In order to determine the geometry of the systems, basic cells containing a single layer of the tested materials were relaxed. In the next step, a two-layer system was created for each of the tested materials. The relaxation results of two layers with 8 atoms in the layer, and a total of 16 atoms in the cell, gave us distances between layers equal 3.6382 Å, 3.5185 Å, and 3.3661 Å for C_3B, graphene, and C_3N, respectively. Once the final coordinates of the pristine bilayer were found, the systems were intercalated with four Li/Na atoms per cell put in the hole sites. The most important parameter describing materials is binding energy. To determine the stability of the tested pristine bilayers, the binding energy value was calculated according to the following formula

$$E_{\text{b.bilayer}} = E_{\text{bilayer}} - 2E_{\text{monolayer}}. \tag{1}$$

The binding energy of Li and Na atoms between the layers was calculated as follows

$$E_{\text{b.Li/Na}} = E_{\text{bilayer.Li/Na}} - E_{\text{bilayer}} - 4E_{\text{Li/Na}}. \tag{2}$$

According to the definitions of binding energies, the negative value of binding energy suggests that the presented bilayer systems are energetically more favorable and stable at temperature 0 K. Table I contains all relevant calculations from the point of view of stability and degeneracy. After Li intercalation, the distance decreases slightly for C_3B and increases slightly for graphene. Na intercalation causes a significant increase in the distance between the layers for both C_3B (19.27%) and graphene (37.68%).

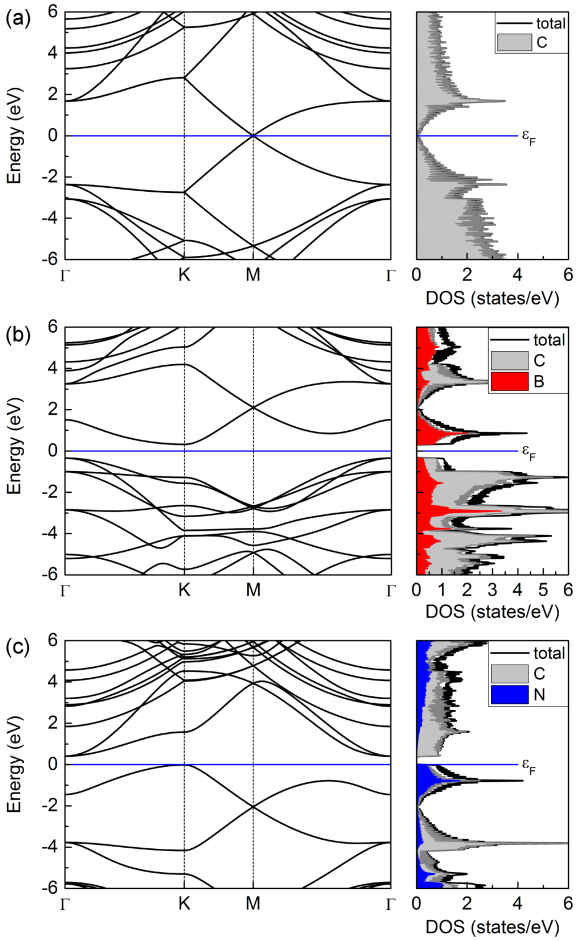

Fig. 2. Electronic band structure with partial density of states (DOS) along the Γ–K–M–Γ high-symmetry line for monolayers: (a) graphene, (b) C_3B, (c) C_3N.

TABLE I

The calculated binding energies ($E_{\text{b.bilayer}}$, $E_{\text{b.Li}}$, and $E_{\text{b.Na}}$) and interlayer distance (d) for pristine bilayer systems and for systems after intercalation by Li/Na atoms.

	C_3B	graphene	C_3N
$E_{\text{b.bilayer}}$ [Ry]	−0.0929	−0.0864	−0.0745
$E_{\text{b.Li}}$ [Ry]	−0.7792	−0.2324	no data avail.
$E_{\text{b.Na}}$ [Ry]	−0.2133	0.3149	no data avail.
d_{pristine} [Å]	3.6382	3.5185	3.3661
$d_{\text{int.Li}}$ [Å]	3.6062	3.5991	no final coord.
$d_{\text{int.Na}}$ [Å]	4.3393	4.8443	no final coord.

Nitrided graphene C_3N can be excluded as a potential anode material because, after Li/Na intercalation, final coordinates were not found.

Calculations of the density of electronic states and the energy gap were made in order to answer the question of whether the investigated structures belong to insulators, semiconductors, semimetals or conductors. That is shown in Fig. 2 and Fig. 3

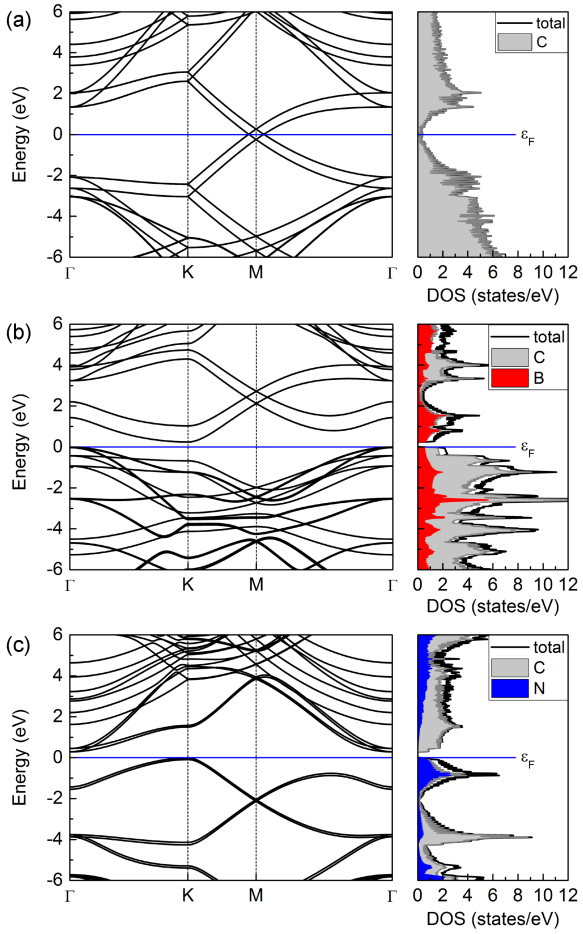

Fig. 3. Electronic band structure with partial density of states (DOS) along the Γ–K–M–Γ high-symmetry line for bilayers: (a) graphene, (b) C_3B, (c) C_3N.

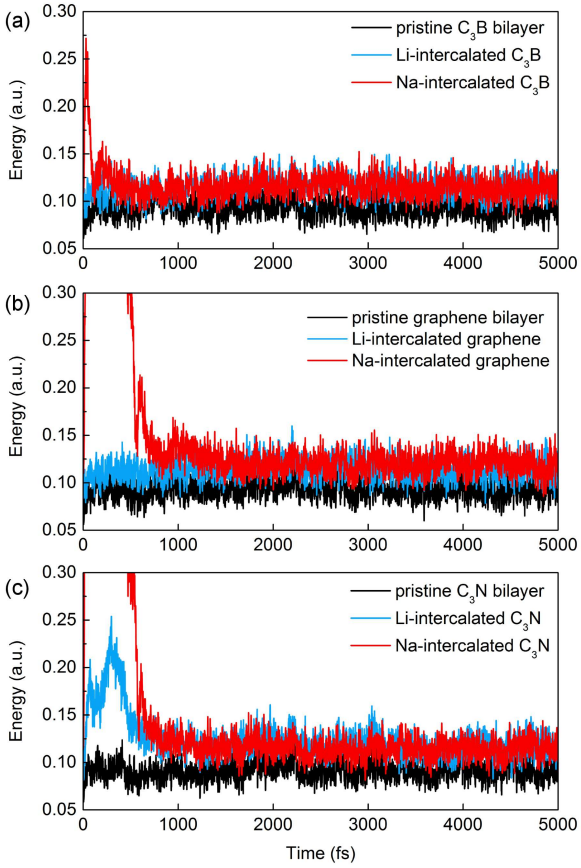

Fig. 4. Kinetic energy of (a) pristine and intercalated C_3B bilayer, (b) pristine and intercalated graphene bilayer, and (c) pristine and intercalated C_3N bilayer as a function of time.

for monolayer and bilayer pristine systems, respectively. As we see, monolayer graphene is semimetal with a Dirac cone at the Fermi level, while bilayer graphene presents a metal character. When it comes to systems with boron or nitrogen, we are dealing with semiconductors with a small band gap.

To explain dynamic stability at room temperature, all materials were investigated with CP2K. Calculations were made for pristine bilayer systems and after Li/Na intercalation. The kinetic energies as a function of time are presented in Fig. 4. All pristine materials show structural stability at room temperature. After intercalation, the C_3B material shows the greatest stability for both lithium and sodium.

4. Conclusions

First-principles calculations based on density functional theory have been carried out to investigate the potential of anode material of two C_3B layers, graphene, and a C_3N system with intercalation of Li and Na atoms. As Quantum Espresso calculations show, all bilayer pristine systems are stable at 0 K. AIMD calculations confirm the stability of pristine at room temperature. In addition, AIMD calculations showed an interesting fact of layer shifting in the case of graphene and C_3B, while C_3N shows a strong attraction between the layers. The distance between the layers is the greatest for the system with boron and the smallest for the one with nitrogen. After Li/Na intercalation, nitrogen systems do not return final coordinates, so the lowest energy ground state cannot be found. In the case of the C_3B system, after lithium intercalation, the distance between the layers slightly decreases by 0.88%, while after intercalation with sodium it significantly increases by 19%. For graphene after lithium intercalation, the increase in the distance between the layers is insignificant by 2.3%, sodium intercalation causes a significant increase in the distance between graphene layers by 37.7%. In the case of the C_3N material, it can be excluded as a potential material in the context of anode construction. In turn, replacing one in four carbon atoms with boron can improve the physical properties of the anode for both lithium and sodium electrolytes.

Acknowledgments

This research was supported in part by PLGrid Infrastructure.

References

[1] A.P. Durajski, R. Szczęśniak, Y. Li, C. Wang, J.-H. Cho, *Phys. Rev. B* **101**, 214501 (2020).

[2] A.P. Durajski, R. Szczesniak, *Phys. Chem. Chem. Phys.* **23**, 25070 (2021).

[3] G.T. Kasprzak, R. Szczesniak, A.P. Durajski, *Comput. Mater. Sci.* **225**, 112194 (2023).

[4] A.P. Durajski, G.T. Kasprzak, *Physica B* **660**, 414902 (2023).

[5] K.S. Novoselov, A.K. Geim, S.V. Morozov, D. Jiang, Y. Zhang, S.V. Dubonos, I.V. Grigorieva, A.A. Firsov, *Science* **306**, 666 (2004).

[6] A.P. Durajski, K.M. Gruszka, P. Niegodajew, *Appl. Surf. Sci.* **532**, 147377 (2020).

[7] A. Khandelwal, K. Mani, M.H. Karigerasi, I. Lahiri, *Mater. Sci. Eng. B* **221**, 17 (2017).

[8] M. Alidoust, M. Willatzen, A.-P. Jauho, *Phys. Rev. B* **99**, 125417 (2019).

[9] A.J. Mannix, X.-F. Zhou, B. Kiraly et al., *Science* **350**, 1513 (2015).

[10] H. Oughaddou, H. Enriquez, M.R. Tchalala, H. Yildirim, A.J. Mayne, A. Bendounan, G. Dujardin, M. Ait Ali, A. Kara, *Prog. Surf. Sci.* **90**, 46 (2015).

[11] G.T. Kasprzak, K.M. Gruszka, A.P. Durajski, *Acta Phys. Pol. A* **139**, 621 (2021).

[12] R. Parr, W. Yang, *Density-Functional Theory of Atoms and Molecules*, Oxford University Press, Oxford 1989.

[13] P. Giannozzi, O. Andreussi, T. Brumme et al., *J. Phys. Condens. Matter* **29**, 465901 (2017).